

and the even- L moments of the polarization distributions) for strong decay and found them to be consistent with zero.

The conclusions that may be drawn from the $\Xi^*(1530)$ analysis described above are (a) the spin must be greater than $\frac{1}{2}$, but need not be more than $\frac{3}{2}$, and (b) the Ξ^* parity is that of a $P_{3/2}$ (or $D_{5/2}$) state rather than of a $D_{3/2}$ (or $F_{5/2}$) state. The comparison of the spin χ^2 values of Table II with the distributions of Fig. 3 and also the comparison of the $P_{3/2}$ and $D_{5/2}$ curves of

Fig. 2 support statement (a). Examination of the parity χ^2 's of Table II (in comparison with Figs. 4 and 5) indicates that the $D_{3/2}$ hypothesis is discriminated against with perhaps a $\leq 3\%$ confidence level and thus supports statement (b).

We express appreciation for contributions made by other members of the Alvarez group in the acquiring and processing of the data discussed here. We thank in particular Deane W. Merrill for his interest in the final stages of analysis.

π^- -Pair Photoproduction below 1 BeV*

J. V. ALLABY,[†] H. L. LYNCH, AND D. M. RITSON

High-Energy Physics Laboratory, Stanford University, Stanford, California

(Received 11 October 1965)

Measurements of the differential cross section for the reaction $\gamma+p \rightarrow \pi^-+\pi^++p$ have been made at several angles for photon energies in the range 550–1000 MeV, using the Stanford Mark III linear accelerator. The π^- were detected and momentum-analyzed using a 90° magnetic spectrometer. It was found that the reaction was dominated by the quasi-two-body photoproduction $\gamma+p \rightarrow \pi^-+N^*$ (1238) especially near the threshold for this process. At low momenta, the π^- were identified by range. At high momenta (> 250 MeV/ c), the contaminating electrons were eliminated by using a lead and scintillation-counter sandwich system. The yields of both π^- and π^+ from hydrogen were measured, and the normalization was obtained by comparison with the known cross sections for $\gamma+p \rightarrow \pi^++n$. Computer calculations of the shapes of the yield curves expected from two-body and three-body production enabled the data to be separated into the two possible states $\gamma+p \rightarrow \pi^-+N^*$ (1238) and $\gamma+p \rightarrow \pi^-+\pi^++p$. Angular distributions and total cross sections are presented.

I. INTRODUCTION

THE photoproduction of pion pairs from protons was first observed by detecting negative pions emitted from a hydrogen target placed in the bremsstrahlung beam of the California Institute of Technology synchrotron.^{1–3} This effect was confirmed at Stanford by Friedman and Crowe.⁴

The first detailed study of the reaction producing the negative pions, $\gamma+p \rightarrow \pi^-+\pi^++p$, was carried out by Bloch and Sands^{5,6} at the California Institute of Technology. They detected the π^- with a magnetic spectrometer and used measurements of single π^+ photoproduction to normalize the π^- yield. We have adopted the same technique, but the high intensity of the Stanford Mark III linear accelerator has enabled us to obtain much more data and to analyze in detail the

shapes of the bremsstrahlung yield curves, giving information on the final state.

A group at Cornell also studied the photoproduction of pion multiplets using a hydrogen-filled diffusion cloud chamber.^{7,8} In this work, the dominant process was found to be $\gamma+p \rightarrow \pi^-+\pi^++p$, and this reaction was analyzed and total cross sections for incident photon energies in the range 400–1000 MeV were obtained. The detailed analysis of this reaction led to the conclusions that the π^+ and π^- play markedly different roles so that the process could not be described by a simple statistical model and that an appreciable fraction of the final state was reached by formation of the two-body system π^-+N^* (1238) with subsequent decay of the N^* into π^++p .

These conclusions were the motivation for our study of this process in further detail, and our analysis of the shape of the π^- yield curves has allowed us to separate out the two-body channel and obtain angular distributions of the π^- in the center of mass for the reaction $\gamma+p \rightarrow \pi^-+N^*$ (1238).

* Research supported by the U. S. Office of Naval Research under Contract Nonr 225 (67).

[†] Present address: CERN, Geneva, Switzerland.

¹ V. Z. Peterson and I. G. Henry, Phys. Rev. **96**, 850 (1954).

² M. Sands, M. Bloch, J. G. Teasdale, and R. L. Walker, Phys. Rev. **99**, 652 (1955).

³ V. Z. Peterson, Bull. Am. Phys. Soc. Ser. II, **1**, 173 (1956).

⁴ R. M. Friedman and K. M. Crowe, Phys. Rev. **105**, 1369 (1957).

⁵ M. Bloch and M. Sands, Phys. Rev. **108**, 1101 (1957).

⁶ M. Bloch and M. Sands, Phys. Rev. **113**, 305 (1959).

⁷ J. M. Sellen, G. Cocconi, V. T. Cocconi, and E. L. Hart, Phys. Rev. **113**, 1323 (1959).

⁸ B. M. Chasan, G. Cocconi, V. T. Cocconi, R. M. Schectman, and D. H. White, Phys. Rev. **119**, 811 (1960).

II. THE EXPERIMENT

The Experimental Equipment

A diagram of the basic experimental equipment is shown in Fig. 1. Electrons from the Stanford Mark III linear accelerator struck a 0.036-cm copper radiator. The beam, containing both electrons and photons, then passed through a ditching magnet, which removed the charged particles from the beam, allowing the photons to pass axially through a cylindrical liquid-hydrogen target 5 cm in diameter and 30 cm long. Negative pions emitted from the target and transmitted through the 90° bend, 112-cm-radius spectrometer were detected by a suitable counter telescope placed at the focal plane, in a well-shielded cave. The spectrometer was supported on a gun-mount which enabled the detection angle, θ to be changed remotely by swinging the gun-mount about its axis which passed through the center of the liquid-hydrogen target.

The photon beam position was continuously monitored by means of a television camera viewing the light spot produced by the photons in a cesium bromide crystal mounted accurately on the downstream window of the hydrogen target vacuum chamber. The beam spot was typically ~ 6 mm in diameter and could be positioned to $\sim \pm 1$ mm. The beam direction was known to within ± 5 mrad.

The liquid-hydrogen target was of the condensation type and was constructed for a previous experiment by Browman⁹ and described in detail by him. One modification made was to attach a thick copper heat strap connecting the target cell, containing liquid-hydrogen under excess pressure of $\sim 1\frac{1}{2}$ atm, to the reservoir containing liquid-hydrogen boiling at atmospheric pressure. This was to ensure that the hydrogen in the target cell did not boil and so produce fluctuation in the effective density of the target.

The magnetic spectrometer has been described in detail elsewhere.¹⁰ In this experiment the entrance

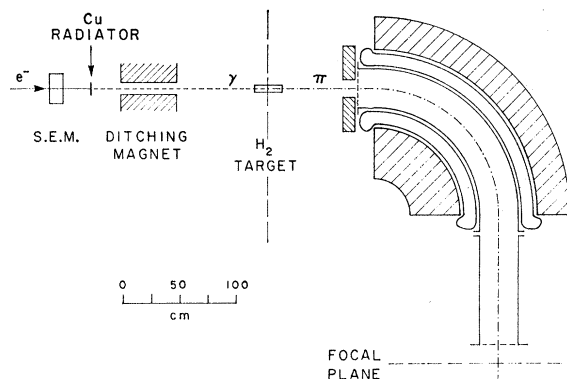


Fig. 1. Schematic diagram of experimental arrangement.

⁹ A. Browman, Ph.D. thesis, Stanford University, Stanford, California (unpublished).

¹⁰ J. V. Allaby and D. M. Ritson, Rev. Sci. Instr. 36, 607 (1965).

aperture was limited by a mask containing a hole 12.7 cm high and 7.6 cm wide, placed about 75 cm from the center of the hydrogen target. Since the spectrometer has no focusing in the nonbend plane, the angular resolution was determined by the size of the defining counter at the focal plane and the size of the entrance aperture. This produced a resolution of ± 15 msr. The intrinsic momentum resolution of the spectrometer is $\pm 0.1\%$, but for this experiment the defining counter was allowed to accept $\pm 1\frac{1}{2}\%$ since high momentum resolution was not necessary.

The counter telescopes used to detect the pions transmitted by the spectrometer had to reject the background of electrons also transmitted. Adequate rejection was obtained by utilizing three different techniques in different momentum ranges. In all cases the defining counter was 7.6×7.6 cm and was preceded by an absorber of suitable thickness to stop protons which were transmitted when the spectrometer was set to detect π^+ mesons.

For the very low momentum measurements, $p_\pi \leq 140$ MeV/c, the pions lost much more energy than electrons in traversing the plastic scintillator; thus good rejection against electrons was obtained by pulse-height discrimination. However, as an additional safeguard, a 5-cm-thick Lucite Čerenkov counter, C, was also used to veto electron events. For this low-momentum range, the telescope was simply two 7.6×7.6 -cm scintillation counters backed up by the Lucite Čerenkov counter. A detected pion was signalled by a $12\bar{C}$ coincidence. With this arrangement the rejection ratio for electrons was typically 300:1.

Figure 2 shows the counter telescopes used in the intermediate- and high-momentum ranges. In the range 120 MeV/c $\leq p_\pi \leq 240$ MeV/c a range telescope was used. A wedge of polyethylene absorber, placed after the proton stopper, was used to compensate for the momentum acceptance of the defining counter and so produce pions with equal momentum. By adjusting the amount of absorber between counters 2 and 3, the pions were made to stop in counter 3. Counter 4 was a veto counter to eliminate electrons. In this arrangement, a

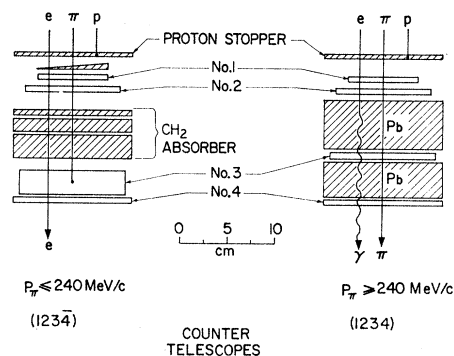


Fig. 2. Two of the counter telescopes used to separate π mesons from electrons.

pion was signalled by a 1234 coincidence. This telescope gave typical rejection ratios against electrons of 100:1.

In the range $p_\pi \geq 240$ MeV/c, the electron contamination was eliminated by using a lead-scintillation counter sandwich. The electrons produced an electromagnetic shower in the lead in which most of the energy was propagated down the telescope in the form of photons. The photons were not detected by the scintillators, and the pions were signalled by 1234 coincidences. The rejection ratio in this momentum range was strongly dependent on the amount of lead in the sandwich which was limited by the range of the pion. At 240 MeV/c the rejection was $\sim 200:1$ but became much better at the higher momenta, being $\sim 2000:1$ at 400 MeV/c.

In all the telescopes, conventional scintillation counters were used which consisted of square sheets of scintillation plastic coupled by Lucite light pipes to R.C.A. 6810A multiplier phototubes. The outputs from the anodes of the phototubes were transmitted on RG-62/U coaxial cable to the counting room. Commercially available Chronetics fast logic was used to determine the coincidence requirements.

The electron beam current was monitored by integrating the output current from two secondary emission monitors in the beam which were periodically calibrated against a Faraday cup although it was not necessary to know the absolute efficiency for this experiment.

The Measurements

The yield of π^- mesons was measured for fixed p_π and θ_π in the laboratory as a function of incident electron energy from threshold up to the maximum energy available (~ 1100 MeV). The machine energy was increased in discrete steps, usually of 50 MeV. Uncertainties in the detection efficiencies of the telescopes were removed by measuring the yield of π^+ mesons at the same p_π from single π^+ photoproduction. The detection efficiency η was then evaluated using published data on the differential cross section for π^+ photoproduction.^{11,12} For the high-momentum runs where the telescope contained many radiation lengths of lead, the data were corrected for the slight difference in interaction lengths of π^+ and π^- . In the worst case this correction was only 5%, and so could be evaluated with some confidence by interpolation from measured π^+ and π^- cross sections,¹³ even though no data exist at exactly the energy region desired. Background runs were taken periodically during the measurement of the yield curve by replacing the liquid-hydrogen target cell by an identical, empty cell, which

was contained in the same vacuum chamber and was moved into the beam line by raising the complete liquid-hydrogen cell and reservoir system. The empty target background was typically $\sim 5\%$ and was subtracted.

The efficiency of the telescopes for detecting electrons was measured by detecting elastically scattered electrons, after removing the copper radiator and degaussing the ditching magnet. In most of the runs, the efficiency for detecting electrons was small enough to make corrections for electron contamination negligible. In a few of the runs in the intermediate momentum range, a small correction was applied which was always less than 10% of the peak yield of π^- .

Yield curves consisting of the number of π^- mesons per incident electron as a function of incident electron energy were obtained at various laboratory angles θ for π^- momenta of 80, 100, 123, 142, 160, 180, 200, 240, 300, 350, 400, and 450 MeV/c. In all, 64 yield curves were obtained of which 7 were cross checks of the results using alternative detection telescopes in the regions where two different telescopes could operate successfully. From the shape of the yield curves, the contribution from $\gamma + p \rightarrow \pi^- + N^*$ was separated out, and 57 measurements of the differential cross section for this process were obtained for effective photon energies between 575 and 950 MeV.

Some measurements were also made of the yield of π^+ mesons above the threshold for π -pair production. Unlike the π^- yield, no sharp rise in yield was seen in the region of N^* production, so it was concluded that the process $\gamma + p \rightarrow \pi^+ + N^{*0}$ was not contributing significantly to the π -pair production, and that we were detecting π^+ mainly from decay of $N^{*++} \rightarrow \pi^+ + p$.

III. THE RESULTS

The dominant production mode of π -pairs was found to be that with the quasi-two-body final state $\pi^- + N^*$ (1238). Hence it was useful to make the analysis follow closely the analysis of single-pion photoproduction, for example $\gamma + p \rightarrow \pi^+ + n$, which was the reaction used to normalize the data.

The measurement of the yield of π^+ mesons at fixed p_π and θ_π from single-pion photoproduction gives the differential cross section $\sigma_+^*(p, \theta)$ in a very simple way, because the kinematics of two-body photoproduction impose a δ function constraint on the energy of the photon (k) initiating the reaction. As a result the yield of π^+ as a function of incident electron energy, E has a shape characterized by the bremsstrahlung function $\Phi(E, k)$ which rises steeply at threshold ($E = k_i$) and then attains an almost constant value when E is about 50 MeV above threshold. Figure 3 shows a typical π^+ yield curve illustrating this feature. The differential cross section can then be related to the height of the yield curve in terms of the detection efficiency, target thickness, radiator thickness, and acceptance of the spectrometer.

¹¹ R. L. Walker, J. G. Teasdale, V. Z. Peterson, and J. I. Vette, Phys. Rev. **99**, 210 (1955). The cross sections used were evaluated from the table of average experimental values of the coefficients A , B , and C in the expansion of $\sigma(\theta)$ in polynomials (Table III of this paper).

¹² F. P. Dixon and R. L. Walker, Phys. Rev. Letters **1**, 458 (1958).

¹³ A. Abashian, R. Cool, and J. W. Cronin, Phys. Rev. **104**, 855 (1956).

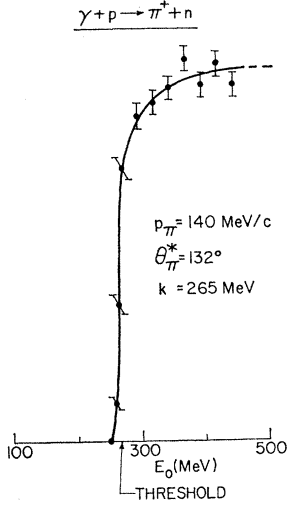


FIG. 3. Illustration of a typical π^+ yield curve.

The situation would be identical for the reaction $\gamma + p \rightarrow \pi^- + N^*$ if it were not for the width of the N^* resonance which necessitates the replacement of the δ function constraint on k by an equivalent Breit-Wigner constraint. However, it is still true that if the measurement of the yield curve of π^- is continued to sufficiently large E , then the yield should attain a constant value which can be directly related to the cross section for producing $N^* + \pi^-$ in a manner similar to the π^+ case.

Thus the qualitative signature of N^* production in the final state is a yield of π^- which rises fairly rapidly in a manner characterized by the N^* mass and width, and becomes independent of E at the higher energies.

Analysis of the Yield Curves

A. π^+ Yield from $\gamma + p \rightarrow \pi^+ + n$

The kinematics of the two-body final state give the following relation for the energy of the photon initiating the reaction:

$$k_i = \frac{1}{2} \left\{ \frac{m_n^2 - (m_p^2 + m_\pi^2) + 2E_\pi m_p}{m_p - E_\pi + p_\pi \cos \theta_\pi} \right\}, \quad (1)$$

where E_π , p_π , and θ_π are the laboratory total energy, momentum, and angle of the detected pion.

The yield of π^+ then depends on the number of photons of energy k_i available at the given electron energy E , which is given by the well-known bremsstrahlung function, $\Phi(E, k)$. We can express the yield of π^+ per electron as

$$Y^+(E) = \Phi(E, k_i) \delta k_i T(\theta) \sigma_+^*(p, \theta) (d\Omega^*/d\Omega) \Delta\Omega \eta(p), \quad (2)$$

where δk_i is the photon energy interval corresponding to the momentum acceptance of the spectrometer $= (dk/dp) \Delta p$; $T(\theta)$ is the H_2 target thickness in protons cm^{-2} . [The angular dependence comes about because the spectrometer sees a length of target which is a function of the angle. $T(\theta) \propto (1/\sin\theta)$ except at angles

$\theta < 35^\circ$.] $\sigma_+^*(p, \theta)$ is the π^+ differential cross section in the center of mass corresponding to production of π^+ with momentum p and angle θ in the laboratory; $(d\Omega^*/d\Omega)$ is the solid angle transformation factor; $\Delta\Omega$ is the solid angle of the detection system; and $\eta(p)$ is the efficiency of the counter telescope when detecting pions of momentum p .

The yield may be expressed in a more convenient form:

$$Y^+(E) = J^+(p, \theta) K(p, \theta) \sigma_+^*(p, \theta) k_i \Phi(E, k_i), \quad (3)$$

where

$$J^+(p, \theta) = (d\Omega^*/d\Omega)(p/k_i)(dk/dp)$$

= Jacobian for π^+ photoproduction;

$$K(p, \theta) = T(\theta)(\Delta p/p)\Delta\Omega\eta(p).$$

In this experiment, Eq. (3) was utilized together with the known value of $\sigma_+^*(p, \theta)$ to evaluate $K(p, \theta)$.

B. π^- Yield from $\gamma + p \rightarrow \pi^- + \pi^+ + p$

The spectrometer in this case measured the yield of π^- per incident electron at fixed p and θ as a function of E . The kinematics of the three-body final state give the following relation:

$$k = \frac{1}{2} \left\{ \frac{r^2 - (m_p^2 + m_\pi^2) + 2E_\pi m_p}{m_p - E_\pi + p_\pi \cos \theta_\pi} \right\}, \quad (4)$$

where k is the energy of the photon initiating the reaction and r^2 is the invariant mass squared of the recoiling $p\pi^+$ system. In analogy with the π^+ photoproduction we define k_i as the photon energy when $r^2 = M^2$, M being the mass of the N^* (1238 MeV). The threshold for production of π -pairs, k_0 is given by Eq. (4) with $r^2 = (m_p + m_\pi)^2$.

From Eq. (4) we see that for every possible value of the invariant mass of the recoiling $p\pi^+$ system there corresponds a definite photon energy to produce a π^- of the correct p and θ . This is an important point because we shall identify the "two-body" cross section for $\gamma + p \rightarrow \pi^- + N^*$ at fixed p and θ with the photon energy k_i corresponding to recoil of invariant mass 1238 MeV. It should be noted, however, that the photon energies initiating the reaction vary as we consider different regions of the mass spectrum of the N^* and are specified through Eq. (4).

In order to describe the yield of π^- we need the probability that the $p\pi^+$ system has invariant mass r^2 as a function of r^2 [or equivalently of k specified through Eq. (4)]. Here we recognize two possible situations. The $p\pi^+$ system can exist in a nonresonant state in which we assume that the invariant mass distribution is dependent only on phase space. On the other hand, the $p\pi^+$ system can be produced in the N^* , and we describe the mass distribution in this case by a P -wave Breit-Wigner resonance multiplied by the phase space. The

probabilities for these two situations are designated $\rho(k)$ and $\rho'(k)$, respectively, and are given by

$$\rho(k) = a(\sin\theta_\pi/kr^2)(p_\pi^3/E_\pi) \times \{[r^2 - (m_p - m_\pi)^2][r^2 - (m_p + m_\pi)^2]\}^{1/2}, \quad (5)$$

$$\rho'(k) = b \frac{\sin\theta_\pi p_\pi^3}{kr^2 E_\pi} \frac{M\Gamma}{(r^2 - M^2)^2 + M^2\Gamma^2}, \quad (6)$$

where

$$\Gamma = \Gamma_0 \left\{ \frac{[r^2 - (m_p - m_\pi)^2][r^2 - (m_p + m_\pi)^2]}{[M^2 - (m_p - m_\pi)^2][M^2 - (m_p + m_\pi)^2]} \right\}^{3/2} \quad (7)$$

= *P*-wave Breit-Wigner width;

Γ_0 is the width of N^* and equals 94 MeV; and a, b are normalization constants chosen such that

$$\int_{k_0}^{\infty} \rho'(k) dk = 1, \quad (8)$$

$$\int_{k_0}^{k_t} \rho(k) dk = \int_{k_0}^{k_t} \rho'(k) dk. \quad (9)$$

The parametrization of the N^* distribution through Eqs. (6) and (7) gives reasonably good agreement with the results of π - p phase-shift analyses, especially within one width from the central value, using Γ_0 of 94 MeV.¹⁴

We can now describe the yield of π^- per incident electron:

$$Y^-(E) = J^-(p, \theta) K(p, \theta) \left[\sigma_{-}^*(p, \theta) \int_{k_0}^E k\Phi(E, k) \rho(k) dk + \sigma_{-}^{*'}(p, \theta) \int_{k_0}^E k\Phi(E, k) \rho'(k) dk \right], \quad (10)$$

where

$J^-(p, \theta) = (d\Omega^*/d\Omega)(p/k_t)(dk/dp) =$ Jacobian for $\gamma + p \rightarrow \pi^- + N^*$ evaluated at central mass value of N^* ;

$$K(p, \theta) = T(\theta) \frac{\Delta p}{p} \Delta\Omega\eta(p);$$

$\sigma_{-}^*(p, \theta)$ is the center-of-mass differential cross section for producing π^- with momentum p and angle θ in the laboratory when recoil π^+p is nonresonant; and $\sigma_{-}^{*'}(p, \theta)$ is the center-of-mass differential cross section for producing π^- with momentum p and angle θ in the laboratory when recoil π^+p is an N^* .

The Jacobian, which has small k dependence, has been pulled out of the integral and evaluated at $k = k_t$ (i.e., assuming recoil of a unique mass of 1238 MeV).

Rewriting Eq. (10) in a simpler form,¹⁵ we have the

following:

$$Y^-(E) = AN(E) + BN'(E), \quad (11)$$

where

$$A = J^-(p, \theta) K(p, \theta) \sigma_{-}^*(p, \theta),$$

$$B = J^-(p, \theta) K(p, \theta) \sigma_{-}^{*'}(p, \theta),$$

and

$$N(E) = \int_{k_0}^E k\Phi(E, k) \rho(k) dk,$$

$$N'(E) = \int_{k_0}^E k\Phi(E, k) \rho'(k) dk.$$

In order to evaluate $\sigma_{-}^{*'}(p, \theta)$, the integrals $N(E)$ and $N'(E)$ were calculated numerically and the coefficients A and B were adjusted to give the best least-squares fit to the measured yield curves. For the purpose of fitting, only statistical errors were assigned to the yield so that the χ^2 probability could be used as a test of the adequacy of our analysis. Since acceptable χ^2 values were obtained for all the yield curves we feel the technique is acceptable even though we have implicitly ignored possible interference between the resonant and nonresonant production. Figure 4(a) shows one of our yield curves with the fitted function $Y^-(E)$. Figure 4(b) shows the "unfolded" yield and displays graphically the invariant mass distributions defined in Eqs. (5) and (6).

From the fitted value of B and its associated error, we obtained $\sigma_{-}^{*'}(p, \theta)$ using the measured π^+ yield at the same p to evaluate $K(p, \theta)$. The error on $\sigma_{-}^{*'}(p, \theta)$ included the fitting error, the error on the π^+ cross section, as well as the statistical errors from both the π^- and π^+ yields.

In order to plot angular distributions we associated

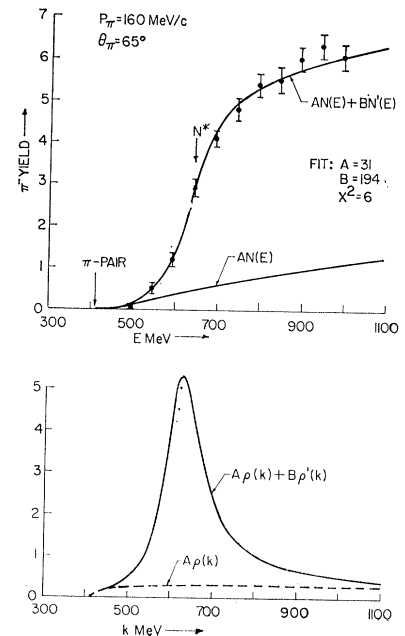


FIG. 4. (a) π^- yield curve showing theoretical fit. (b) The same theoretical fit after unfolding the bremsstrahlung spectrum. The symbols are explained in the text.

¹⁴ P. Finkler, University of California Radiation Laboratory (private communication).

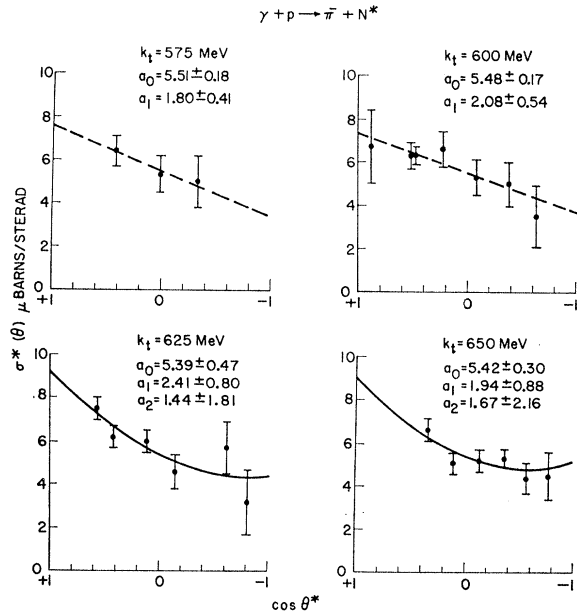


FIG. 5. Angular distributions of π^- in the center-of-mass system for $\gamma + p \rightarrow \pi^- + N^*$ for photon energies of 575, 600, 625, and 650 MeV.

the cross section $\sigma_{-}^*(p, \theta)$ with the two-body cross section $\sigma^*(\theta)$ at fixed photon energy, k_t , in analogy with single-pion photoproduction. The center-of-mass differential cross sections for $\gamma + p \rightarrow \pi^- + N^*$ as a function of $\cos \theta^*$ are shown in Figs. 5-7, for values of k_t from 575 to 950 MeV.

The differential cross sections were fitted by the

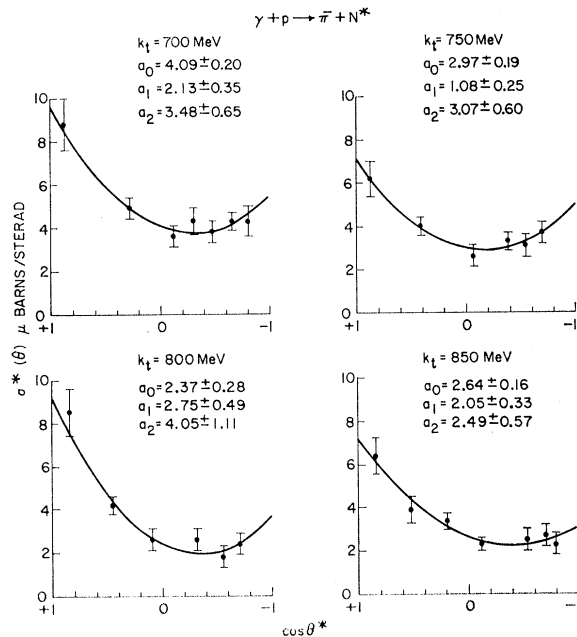


FIG. 6. Angular distributions of π^- in the center-of-mass system for $\gamma + p \rightarrow \pi^- + N^*$ for photon energies of 700, 750, 800, and 850 MeV.

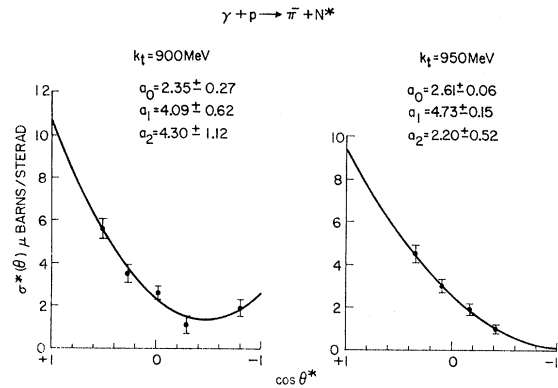


FIG. 7. Angular distributions of π^- in the center-of-mass system for $\gamma + p \rightarrow \pi^- + N^*$ for photon energies of 900 and 950 MeV.

method of least squares by polynomials of the form

$$\sigma^*(\theta) = \sum_{n=0}^l a_n \cos^n \theta^*. \quad (12)$$

The highest power of $\cos \theta^*$ was determined from observation of the χ^2 probability of the fit for different values of l . If l were chosen too large then the χ^2 was too small. The angular distributions for $k_t = 575$ and 600 MeV were well fit with $l=1$. All the other curves were successfully fitted with $l=2$. The fitted coefficients, together with their standard deviation error, are given in Figs. 5-7, which also have the best-fit curves drawn through the data. The total cross section for $\gamma + p \rightarrow \pi^- + N^*$ was evaluated by integration of the differential cross section, using the best-fit coefficients and their associated variances and covariances.

The nonresonant production of π^- has no simple analogy with the two-body single photoproduction, since there is no preferred value for the invariant mass of the recoil $p\pi^+$ system, and so the higher the energy of the incident photons, the greater is the invariant mass of the recoil. Since the probability of producing an invariant mass r^2 is almost independent of r^2 , there is no simple normalization for $\rho(k)$. However, in order to obtain a value for the cross section for $\gamma + p \rightarrow \pi^- + \pi^+ + p$ including both N^* production and nonresonant production, we have used the normalization given by Eq. (9). The physical interpretation of this normalization is that we associate the process with the photon energy k_t , and we have normalized such that we have equal probability for producing recoil-invariant mass greater than or less than the N^* mass, the total probability being unity. With this normalization we can identify $A+B$ with the differential cross section for $\gamma + p \rightarrow \pi^- + \pi^+ + p$, and hence obtain the total-integrated cross section for comparison with earlier data.

The cross sections as a function of photon energy for both $\gamma + p \rightarrow \pi^- + \pi^+ + p$ (including N^* production) and for $\gamma + p \rightarrow \pi^- + N^*$ are shown in Fig. 8, together with

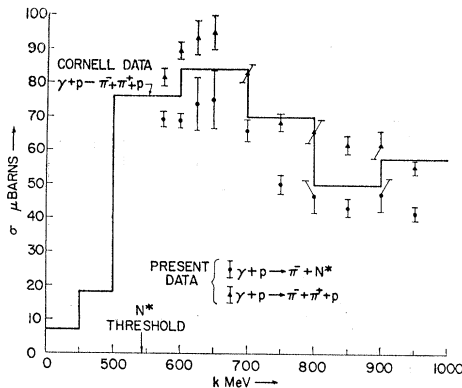


FIG. 8. Cross sections for $\gamma + p \rightarrow \pi^- + N^*$ and $\gamma + p \rightarrow \pi^- + \pi^+ + p$ (all channels) from our results together with the results of Ref. 8.

the histogram from the results of the Cornell group for $\gamma + p \rightarrow \pi^- + \pi^+ + p$.⁸

IV. CONCLUSIONS AND COMPARISONS WITH OTHER EXPERIMENTS

The experiment seems to be in excellent agreement with the early results from diffusion cloud chamber measurements,^{7,8} and the results reported from the Cambridge Bubble Chamber Group.¹⁵

Photo pair production of π mesons proceeds at threshold predominately through the $\pi^- + N^*$ channel. The cross section rises rapidly at threshold, peaks in the

¹⁵ Cambridge group report to the Hamburg Conference, June 1965 (unpublished).

region of 650 MeV, and drops slowly at higher energies. The angular distributions are relatively flat in the neighborhood of threshold and become increasingly forward-peaked at higher energies. The peak of the cross section does not coincide with the position of the second resonance. A possible explanation is that, as in inelastic pion scattering, there is a substantial contribution from the P_{11} state in the region from 600 to 700 MeV. As both the D_{13} and P_{11} intermediate states lead to isotropic angular distributions for the $\pi^- N^*$ final state, it is not readily possible to differentiate between these two possibilities.

In view of the presence of the states $P_{1/2}$, $P_{3/2}$, and $F_{5/2}$ plus retardation terms in photoproduction,¹⁶⁻¹⁸ we have not attempted any detailed analysis of our angular distributions. The results could be explained, however, by a strong P_{11} contribution at threshold with increasing contributions from retardation terms at higher energies.

ACKNOWLEDGMENTS

We wish to acknowledge the help received from E. Burfine with the computer programs used in analyzing the data, many informative discussions of our results with F. Chilton, and the excellent cooperation of the Mark III accelerator crew who made this experiment possible.

¹⁶ L. D. Roper, Phys. Rev. Letters **12**, 340 (1964).

¹⁷ P. Auvil, C. Lovelace, A. Donnachie, A. T. Lea, Phys. Letters **12**, 76 (1964).

¹⁸ P. Bareyre, C. Brickman, A. V. Stirling, and G. Villet, Phys. Letters **18**, 342 (1965).

Search for the Decay $\eta \rightarrow \pi^0 + e^+ + e^-$

D. BERLEY, E. L. HART, D. C. RAHM, D. L. STONEHILL, B. THEVENET,§
W. J. WILLIS,|| AND S. S. YAMAMOTO**

Brookhaven National Laboratory, Upton, New York

(Received 13 October 1965)

A search has been made for the decay $\eta \rightarrow \pi^0 + e^+ + e^-$, which should be very rare if C is conserved in strong and electromagnetic interactions. We have found no events consistent with this decay in a sample of η produced in the reaction $K^- + p \rightarrow \Lambda + \eta$. The upper limit for this decay, at the 90% confidence level, is $R = (\eta \rightarrow \pi^0 + e^+ + e^-) / (\eta \rightarrow \gamma + \gamma) < 0.047$.

I. INTRODUCTION

THE failure of CP (charge conjugation times parity) conservation in the decay of long-lived K^0 mesons into two pions¹ has stimulated interest in

* Work performed under the auspices of the U. S. Atomic Energy Commission.

§ Present address: L.P.C.H.E., Centre d'Etudes Nucleaires de Saclay, Gif-sur-Yvette, Seine-et-Oise, France.

|| Present address: Yale University, New Haven, Connecticut.

** Present address: University of Massachusetts, Amherst, Massachusetts.

¹ J. Christenson, J. Cronin, V. Fitch, and R. Turlay, Phys. Rev. Letters **13**, 138 (1964).

tests of C conservation in strong and electromagnetic interactions.^{2,3} One test which has been suggested⁴ makes use of the fact that the electromagnetic decay

$$\eta^0 \rightarrow \pi^0 + e^+ + e^- \quad (1)$$

is forbidden to first order in the electromagnetic

² J. Prentki and M. Veltman, Phys. Letters **15**, 88 (1965); S. L. Glashow and C. M. Sommerfield, Phys. Rev. Letters **15**, 78 (1965).

³ T. D. Lee and L. Wolfenstein, Phys. Rev. **138**, B1490 (1965).

⁴ J. Bernstein, G. Feinberg, and T. D. Lee, Phys. Rev. **139**, B1650 (1965); M. Nauenberg, Physics Letters **17**, 329 (1965).